Eur. Phys. J. B **5**, 663–669 (1998)

THE EUROPEAN PHYSICAL JOURNAL B

Solidification in the one-dimensional model for a disordered binary alloy under diffusion*

X. Feng, E. Brener[a], D. Temkin, Y. Saito[b] and H. Müller-Krumbhaar

Institut für Festkörperforschung, Forschungszentrum Jülich, 52425 Jülich, Germany

Received: 12 February 1998 / Accepted: 17 April 1998

Abstract. The propagation of the solidification front of a binary alloy growing from its melt is studied by Monte-Carlo simulation and by analytical approximation methods. The simulation shows that in the one-phase region the alloy grows steadily with a velocity controlled solely by kinetics. In the two-phase region, the previously reported anomaly for the diffusionless growth is removed by the diffusion of atoms and the diffusional $t^{1/2}$ growth law is confirmed at least in the range where the diffusionless process is slower than diffusion. We cannot rule out, however, that the anomaly occurring in the diffusionless case persists even under diffusion, when the diffusionless growth asymptotically is faster than a typical diffusion process. The Monte-Carlo simulations are compared with an approximate analytical description ignoring correlations between the components.

PACS. 81.10.-h Methods of crystal growth; physics of crystal growth – 66.30.Dn Theory of diffusion and ionic conduction in solids – 05.40.+j Fluctuation phenomena, random processes, and Brownian motion

1 Introduction

The growth of a binary alloy from its melt is controlled not only by the temperature but also by the concentration of the mother phase, and novel aspects appear in comparison to a single-component system. In the usual treatment of solution growth one considers the diffusional redistribution of components and assumes linear kinetics at the interface such that the growth rate is proportional to the deviation of the concentration at the interface from its equilibrium value. Here we consider the microscopic problem of a disordered AB-alloy [1–3]. Each species of atoms can change its state from liquid to solid during solidification as the interface between the phases is advancing towards the liquid. Without allowing for diffusion, the positions of the atoms however are assumed to be fixed, so that no rearrangement can occur. This corresponds to a very rapid solidification, as, for example, achievable during the formation of metallic glasses. The transition probabilities of this process of an advancing interface should reproduce the equilibrium phase diagram with three regions; the solid, the liquid and the two-phase coexistence, as shown in Figure 1. If the initially liquid melt is suddenly cooled down to a temperature corresponding to the solid one-phase region for the corresponding relative AB-concentration, the stable solid grows steadily with a constant speed. The situation changes if the melt is cooled down into the two-phase coexistence region of the corresponding equilibrium phase-diagram. The process then becomes unsteady with time-dependent growth rate. The spatial regions of the alloy with concentrations close to the solidus line can solidify but the other parts with concentrations close to the liquidus line react as an obstacle to the solidification front and stop the solidification front. Thus the propagation of the solidification front becomes pinned by the fluctuations in the concentration.

Previously we studied the front propagation in the one-dimensional system when the atomic configuration is quenched, *i.e.* without allowing for a rearrangement of atoms. We found that in the two-phase region the interface does not grow steadily but shows an anomalous time dependence [4].

The interface position, h, varies like t^{ν_1} as a function of time t with an exponent ν_1 which depends on the concentration. In a two-dimensional system with one-dimensional interface, similar asymptotics is found for a quenched system in the limit of the large energy of kink formation and finite width of the system [5]. The anomalous behavior is explained by relating the present model to the randomly directed walk [6–12]. A similar relation is also found recently for the driven ratchets [13].

In reality, however, atoms are not completely quenched but are moving and the concentration follows the diffusion law. The natural question then is how the diffusion affects the motion of the interface. We address this question by the Monte-Carlo simulation of the one-dimensional

* Dedicated to J. Zittartz on the occasion of his 60th birthday

[a] e-mail: `E.Brener@fz-juelich.de`

[b] *Permanent address*: Dept of Physics, Keio University 3-14-1 Hiyoshi, Kohoku-Ku, Yokohama 223, Japan.

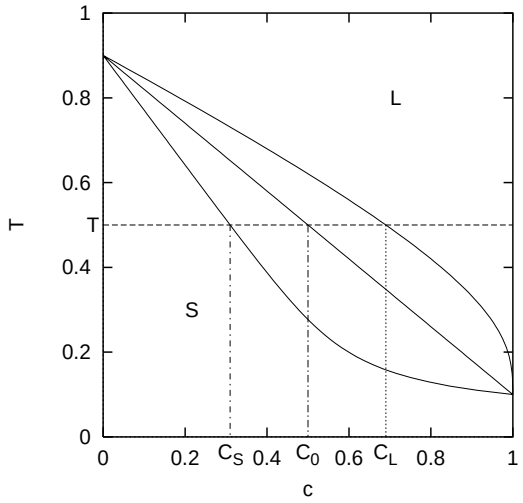

Fig. 1. Phase diagram of an ideal solution.

system and compare the results with an approximate analysis which neglects the correlations in the concentration distribution. We found that if the growth is controlled by the diffusion of the alloy atoms, the anomalous propagation of the interface crosses over to the $t^{1/2}$ law in the two-phase region, at least for the situation, where the quenched system would grow with a smaller exponent than the diffusion exponent $\nu_1 < 1/2$. In the one-phase region on the other hand steady growth is obtained and controlled always by the kinetics of the advancing interface.

2 Model

We consider a binary alloy system composed of atomic species of A and B, and denote the concentration of B atoms by c. Each atom can be either in solid or liquid state. The pure A(B) system solidifies at the temperature $T_A(T_B)$ with the specific latent heat $L_A(L_B)$. We assume that the A and B atoms mix ideally. There is no mixing energy but only a mixing entropy. Then the equilibrium phase diagram is obtained with the solidus line $C_S(T)$ and the liquidus line $C_L(T)$ as

$$C_S(T) = \frac{1 - e^{-\mu_A/T}}{e^{-\mu_B/T} - e^{-\mu_A/T}},$$
$$C_L(T) = \frac{(1 - e^{-\mu_A/T})e^{-\mu_B/T}}{e^{-\mu_B/T} - e^{-\mu_A/T}}. \quad (1)$$

Here the chemical potential difference between the liquid and the solid state for a pure A-atom system is given as $\mu_A = L_A(1 - T/T_A)$ and the corresponding expression for μ_B. Temperature T is measured in units of energy.

At a sufficiently high temperature the system with concentration c is completely molten in the liquid phase. By cooling the system into the solid one-phase region or into the two-phase coexistence region it starts to solidify. We consider here the simplest case of a one-dimensional system, noting that it remains relevant also for the higher-dimensional cases [5] in certain parameter-ranges. Every lattice site on the chain is occupied by an atom of either A or B species. We introduce the state variable n_i which assumes the value zero or unity according to whether the site i is occupied by an A or B atom respectively. The average of n_i over the whole lattice sites L should be the given concentration c:

$$c = \frac{1}{L}\sum_{i=1}^{L} n_i. \quad (2)$$

On this chain we assume a single interface which separates the solid and liquid phases, for example, solid to the left and liquid to the right. The interface position h is defined then as the lattice site of the rightmost solid atom. It can be either a species of A or B. If it melts the interface-height decreases by one: $h \to h - 1$. If the liquid atom to the right of the interface solidifies, the interface advances by one: $h \to h + 1$. The interface motion is assumed to take place stochastically following the master equation

$$\frac{\partial P(h,t)}{\partial t} = W(h+1 \to h)P(h+1,t) - [W(h \to h+1) + W(h \to h-1)]P(h,t) + W(h-1 \to h)P(h-1,t) \quad (3)$$

where $P(h,t)$ is the probability that the interface is at a site h at time t. The transition probabilities W depend on the atomic configurations around the interface. We consider a model where the transition probability W depends only locally on the type of particle which changes its state during melting or solidification. If the solid site h is occupied by an X (= A or B) atom and the liquid site $h+1$ by a Y (= A or B) atom, the transition probability of the interface advancement is given as

$$W(h \to h+1) = w_{+Y} \quad (4)$$

and that of the interface retardation as

$$W(h \to h-1) = w_{-X}. \quad (5)$$

The detailed balance condition requires that the kinetic ratio w_{-X}/w_{+X} should be equal to the one $\exp(-\mu_X/T)$ determined by the thermodynamics:

$$\frac{w_{-X}}{w_{+X}} = e^{-\mu_X/T} \quad (6)$$

where X = A or B.

If the interface motion is so fast that there is no time for the atomic configurations to change while the interface traverses the whole system, the configuration can be regarded as being quenched. In reality the atoms are moving and the configuration changes according to the diffusion law;

$$\frac{\partial Q(\{n\},t)}{\partial t} = \sum_{\delta=\pm1} W_D(n'_i, n'_{i+\delta} \to n_i, n_{i+\delta})Q(\{n'\},t) - \sum_{\delta=\pm1} W_D(n_i, n_{i+\delta} \to n'_i, n'_{i+\delta})Q(\{n\},t) \quad (7)$$

where $Q(\{n\},t)$ is the probability to find the atomic configuration $\{n\}$ at a time t. The configurations $\{n'\}$ are different from the configurations $\{n\}$ by the exchange of states at the site i and its neighbor $i+\delta$. Here we assume a simple diffusion such that the transition probabilities W_D are constant and equal to the diffusion coefficient. In principle the diffusion coefficient in the solid, D_S, is different from that of liquid D_L. In this paper two typical cases are considered: the symmetric diffusion where $D_S = D_L$, and the one-sided diffusion where $D_S = 0$.

3 Monte-Carlo simulation

The motion of the interface is simulated by the Monte-Carlo method. In the simulation, in principle, all the atoms in the chain have the possibility to move stochastically but the influence upon the interface motion is localized within the diffusion length $D_{S(L)}/v$ near the interface, when the interface is moving with the instantaneous velocity v. In the two-phase region the asymptotic velocity is expected to vanish but within our simulation time less than 10^5 one obtains a finite velocity. In order to save computing time we allow the diffusion of atoms within ranges of l_S and l_L from the interface in the solid and liquid phases respectively which are chosen sufficiently larger than the diffusion lengths.

The simulation proceeds as follows. Let the interface be located at a site h between a solid X and a liquid Y atom, where both X and Y can be either of type A or B. After the time increment of $\Delta t = 1/(w_{-X}+w_{+Y}+D_S l_S + D_L l_L)$, the interface advances forward with a probability $\Delta t w_{+Y}$, it recedes backward with a probability $\Delta t w_{-X}$, and one of the solid (liquid) atoms in the range l_S (l_L) from the interface exchanges its position with its neighbor solid (liquid) atom with a probability $\Delta t D_S$ ($\Delta t D_L$).

Parameters are chosen to be the same as those in the previous work [4] for comparison; $T_A = 0.9, T_B = 0.1, L_A/T_A = L_B/T_B = 1, T = 0.5$ and $w_{+A} = w_{+B} = 1$. Thus the equilibrium concentrations are $C_S = 0.310$ and $C_L = 0.690$, and the melting probabilities are $w_{-A} = e^{-0.8} = 0.4493$, and $w_{-B} = e^{0.8} = 2.226$. The new parameters in the present study are the diffusion constants D_S and D_L. They are chosen as $D_S = D_L = 1$ for the symmetric diffusion and $D_S = 0, D_L = 1$ for the one-sided diffusion. The system size is chosen such that it is sufficiently larger than the displacement of the interface. The range of diffusion is chosen in the largest case as $l_S = l_L = 1500$.

From the simulation we calculate the interface mean displacement $\langle h(t)\rangle$ and its variation $\sigma(t) \equiv \sqrt{\langle (h(t) - \langle h(t)\rangle)^2\rangle}$. Here $\langle A\rangle$ means the sample average of the quantity A over at least 100 samples simulated. Their time variations are shown in Figure 2 in the case with the symmetric diffusion and in Figure 3 in the case with the one-sided diffusion.

They depend on time asymptotically in power laws; $\langle h(t)\rangle \sim t^{\nu_1}$ and $\sigma(t) \sim t^{\nu_2}$. The estimated exponents ν_1 and ν_2 are shown in Figure 4. In the diffusionless case ($D_S = D_L = 0$) [4] our model can be mapped to the

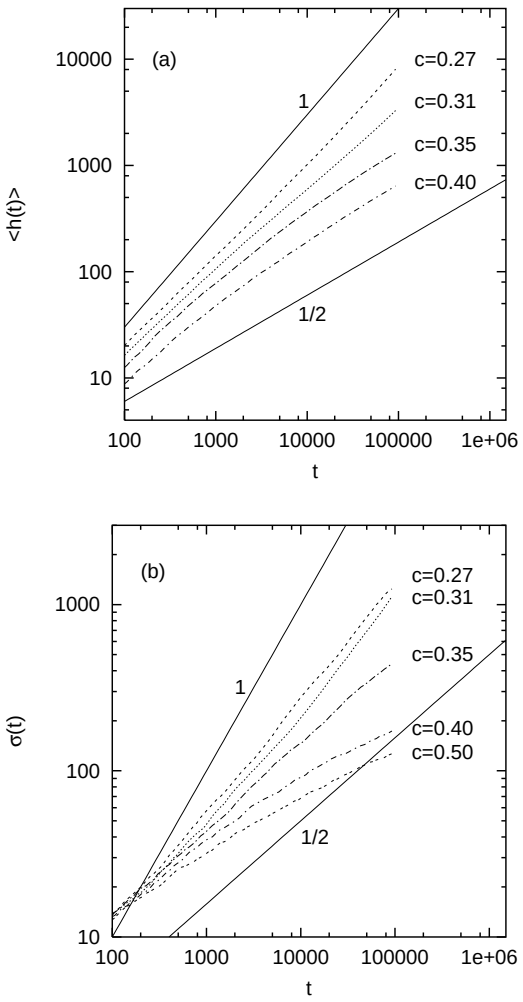

Fig. 2. Time evolution of (a) the interface position $\langle h(t)\rangle$ and (b) its width $\sigma(t)$ for the symmetric diffusion model. Two straight solid lines represent the asymptotic behavior with exponent 1 and 1/2.

directed random walk with a waiting time distribution for forward interface jumps $F(\tau) \sim \tau^{-(1+\gamma)}$ with $\gamma = 1.25\ln(c^{-1}-1)$, where the exact behavior of ν_1 and ν_2 are known [6–12]

$$\begin{aligned} \nu_1 = 2\nu_2 = 1 \quad &\text{for} \quad 0 < c < c_2 = 0.168, \\ \nu_1 = 1, 2\nu_2 = 3-\gamma \quad &\text{for} \quad c_2 < c < C_S, \\ \nu_1 = \nu_2 = \gamma \quad &\text{for} \quad C_S < c < 0.5. \end{aligned} \tag{8}$$

These exact results for the diffusionless growth are also shown in Figure 4 as solid and dashed lines.

In the diffusionless growth the exponent ν_2 increases anomalously above 1/2 in the concentration range $c_2 < c < c_3 = 1/(1+e^{0.4}) \approx 0.401$ due to the strong pinning effect of B atoms. With diffusion the anomalous increment of the interface width seems to be healed such that ν_2 becomes closer to 1/2. The reason might be that the large cluster of B atoms which pins the solidification front will be resolved by the diffusion of B atoms.

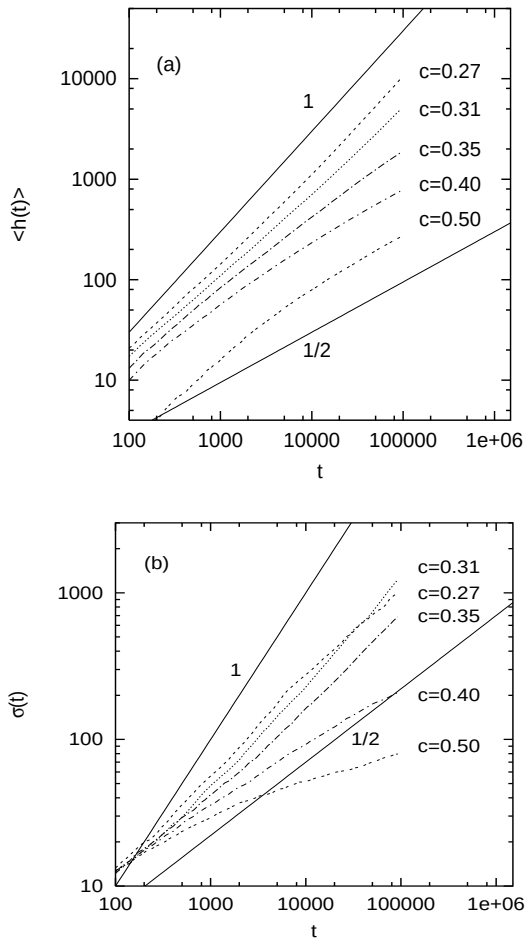

Fig. 3. Time evolution of (a) the interface position $\langle h(t)\rangle$ and (b) its width $\sigma(t)$ for the one-sided diffusion model. Two straight solid lines represent the asymptotic behavior with exponent 1 and 1/2.

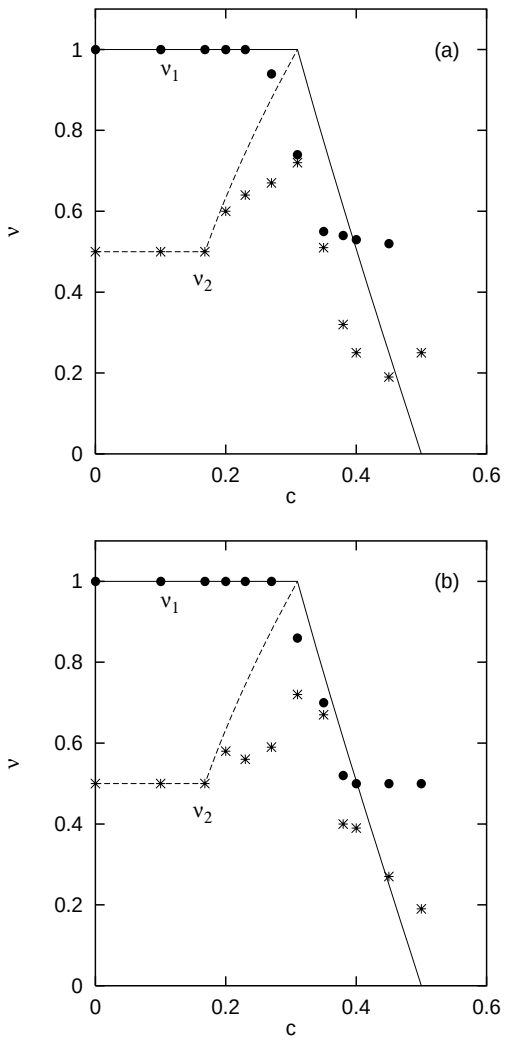

Fig. 4. Exponent ν_1 for the interface position and ν_2 for its width *versus* the B-atom concentration c for (a) symmetric diffusion model and (b) one-sided diffusion model. Solid and dashed lines are the exact diffusionless behaviors of ν_1 and ν_2, respectively. The symbol dots and stars represent the estimated ν_1 and ν_2 from the Monte-Carlo simulation with diffusion, respectively.

Close to $c = 0.5$ the exponent ν_2 seems to remain smaller than 1/2 even with diffusion as in the case without diffusion. Concerning the exponent ν_1 for the mean displacement one can observe that it takes the value close to 1/2 in the region $c_3 < c < 0.5$ and remains larger than 1/2 in the region $C_S < c < c_3$ at least in our time limited simulations. This result can be understood by the approximate analysis in the next section if the growth is controlled by the diffusion.

4 Coarse-grained description of the diffusion-limited solution growth

Temkin [3] derived effective diffusion equations and the boundary conditions for the averaged concentration fields $c_L(x,t)$ and $c_S(x,t)$ in the frame of reference of the moving interface. Those equations have been derived by neglecting the correlations of the concentrations in different spatial points such that $c(x,x',t) = c(x,t)c(x',t)$ where $c(x,t)$ is the probability to find atom B at the position x and time t; $c(x,x',t)$ is the probability to find atoms B at the positions x and x' at the same time t. The equations are [3]

$$\frac{\partial c_S(x,t)}{\partial t} = D_S^e \frac{\partial^2 c_S}{\partial x^2} + v\frac{\partial c_S(x,t)}{\partial x} \quad \text{for} \quad x \le 0$$
$$\frac{\partial c_L(x,t)}{\partial t} = D_L^e \frac{\partial^2 c_L}{\partial x^2} + v\frac{\partial c_L(x,t)}{\partial x} \quad \text{for} \quad x \ge 0 \quad (9)$$

where the interface velocity is $v(t) = d\langle h(t)\rangle/dt$;

$$D^e_{S(L)} = D_{S(L)} + \frac{1}{2}\Big[w_{+A} + (w_{+B} - w_{+A})c_L(0,t) + w_{-A} + (w_{-B} - w_{-A})c_S(0,t)\Big] \quad (10)$$

are the effective diffusion coefficients which differ from the usual diffusion coefficients D_S and D_L due to the interface fluctuations. The initial distribution of components is uniform and random, $c_{S(L)}(x,0) = c$ and $c_{S(L)}(x,x',0) = c^2$. Far from the interface the concentration is kept to c of the mother phase:

$$c_S(-\infty,t) = c_L(\infty,t) = c. \tag{11}$$

The velocity of the solid-liquid interface is kinetically determined as the difference of the solidification and the melting rate:

$$\begin{aligned} v(t) = w_{+A} + (w_{+B} - w_{+A})c_L(0,t) \\ - w_{-A} - (w_{-B} - w_{-A})c_S(0,t). \end{aligned} \tag{12}$$

Also the material conservation at the interface relates the flux of B atoms at the interface as

$$\begin{aligned} vc_L(0) + D_L^e \frac{\partial c_L}{\partial x} &= vc_S(0) + D_S^e \frac{\partial c_S}{\partial x} \\ &= w_{+B}c_L(0) - w_{-B}c_S(0). \end{aligned} \tag{13}$$

If the steady state $\langle h(t)\rangle = vt$ is realized ($0 < c < C_S$), $\partial c_{S(L)}/\partial t = 0$ and we obtain the velocity

$$v = \frac{w_{+A}w_{+B} - cw_{+A}w_{-B} - (1-c)w_{-A}w_{+B}}{cw_{+A} + (1-c)w_{+B}}\,. \tag{14}$$

The value is determined only by the kinetics ($w_{\pm A,B}$) and agrees with the exact velocity for the diffusionless growth [1].

The front velocity (14) remains finite only in the one-phase solid region but it vanishes at the solidus line C_S. In the two-phase region the steady growth with a finite velocity is impossible and it follows from this sets of equations (9–13) that the interface moves asymptotically in proportion to $t^{1/2}$ [3]. For an arbitrary time we can numerically integrate the set of equations (9–13) and obtain the motion of the interface $\langle h(t)\rangle$. Time dependence of the interface position obtained by numerical integration is compared with that obtained by Monte-Carlo simulation in Figure 5. For example for the symmetric diffusion model ($D_S = D_L = 1$) at the concentration $c = 0.35$ in Figure 5a the numerical integration gives a position $\langle h(t)\rangle$ in excellent quantitative agreement with the Monte-Carlo result. A similar quantitative agreement is found for both the one-sided diffusion model and the symmetrical model at the concentration $c = 0.40$ as shown in Figure 5b and d. At the concentration $c = 0.50$ for the symmetrical model the interface does not move in average $\langle h(t)\rangle = 0$. For the one-sided model the Monte-Carlo data for the initial interface motion still agree with numerical integration with the effective diffusion coefficients. However, for larger time the data agree with the numerical integration with bare diffusion constants, $D_S = 0$ and $D_L = 1$, rather than that with the effective ones, D_S^e and D_L^e, as shown in Figure 5e.

For the one-sided diffusion model at $c = 0.35$ in Figure 5c, the Monte-Carlo data still agree with numerical integration during some initial time but we observe a deviation increasing in time, and even bigger deviations from the results obtained with bare diffusion constants. So far from these data for $c = 0.35$ and our long but limited simulation times we cannot make a clear statement if the exponent ν_1 approaches to the diffusionless value $\nu_1 \approx 0.77$ or the diffusional value $\nu_1 = 1/2$, or even some other nontrivial value! We will come back to this point in the conclusion.

The given effective description does not take into account the correlation of concentration between different spatial points. Indeed those correlations are absent in the initial distribution of atoms in our chains and their formation requires some time. We think that this explains the fact that all our Monte-Carlo data agree well with the results based on the effective equations for the small time where nontrivial correlations have not yet built up.

It is clear that correlations become smaller with an increase of the diffusion coefficients and thus the time when the deviation from the correlationless description starts should increase. Qualitatively we can see this effect from the different data for $c = 0.35$. Agreement for the symmetrical model ($D_S = D_L = 1$, Fig. 5a) holds for all our simulation time while for the one-sided model ($D_S = 0, D_L = 1$, Fig. 5c) the increasing deviation can be observed already at $t \cong 10^3$.

The other parameters which affect the correlations are $(w_{+B} - w_{+A})$ and $(w_{-B} - w_{-A})$. The correlations (together with two-phase region) disappear when both parameters are zero. We have performed the Monte-Carlo simulations without diffusion for two sets of the parameters $w_{+B} = w_{+A} = 1$, $w_{-B} = 1/w_{-A} = 2.226$, $c = 0.35$ (Fig. 6a) and $w_{+B} = w_{+A} = 1$, $w_{-B} = 1/w_{-A} = 1.4$, $c = 0.435$ (Fig. 6b). The parameters are so chosen that the exponents ν_1 of the interface position in the above two diffusionless cases are the same and are around 0.77 from the formula $\nu_1 = \ln\left(\frac{1-c}{c}\right)/\ln(w_{-B})$ [8]. In the second case the parameter $(w_{-B} - w_{-A})$ is smaller and one can see that the deviation of the Monte-Carlo data from the effective description starts later. It is interesting to note that even without diffusion the initial behavior can be described by the system of effective diffusion equations with diffusion coefficients which come only from the interface fluctuations.

For the two-phase region in the long-time asymptotics the system goes to equilibrium (even without diffusion) and correlations decay. However, the asymptotic behavior of the interface velocity which also goes to zero still depends on these small correlations. For example for $c = 0.5$ the dependence $\langle h(t)\rangle$ on t deviates substantially from the dependence calculated without correlations. It seems that the asymptotic behavior can be described by bare diffusion constants rather than by effectives ones (Fig. 5e). We think that the correlations renormalize the effective diffusion coefficients back to the bare ones. The description with bare diffusion constants should exactly correspond to the system without interface fluctuations. As can be seen from the Figure 2 and Figure 3 the variation $\sigma(t)$ for $c = 0.5$ grows slower than $t^{1/2}$ which means that the interface fluctuations are indeed small.

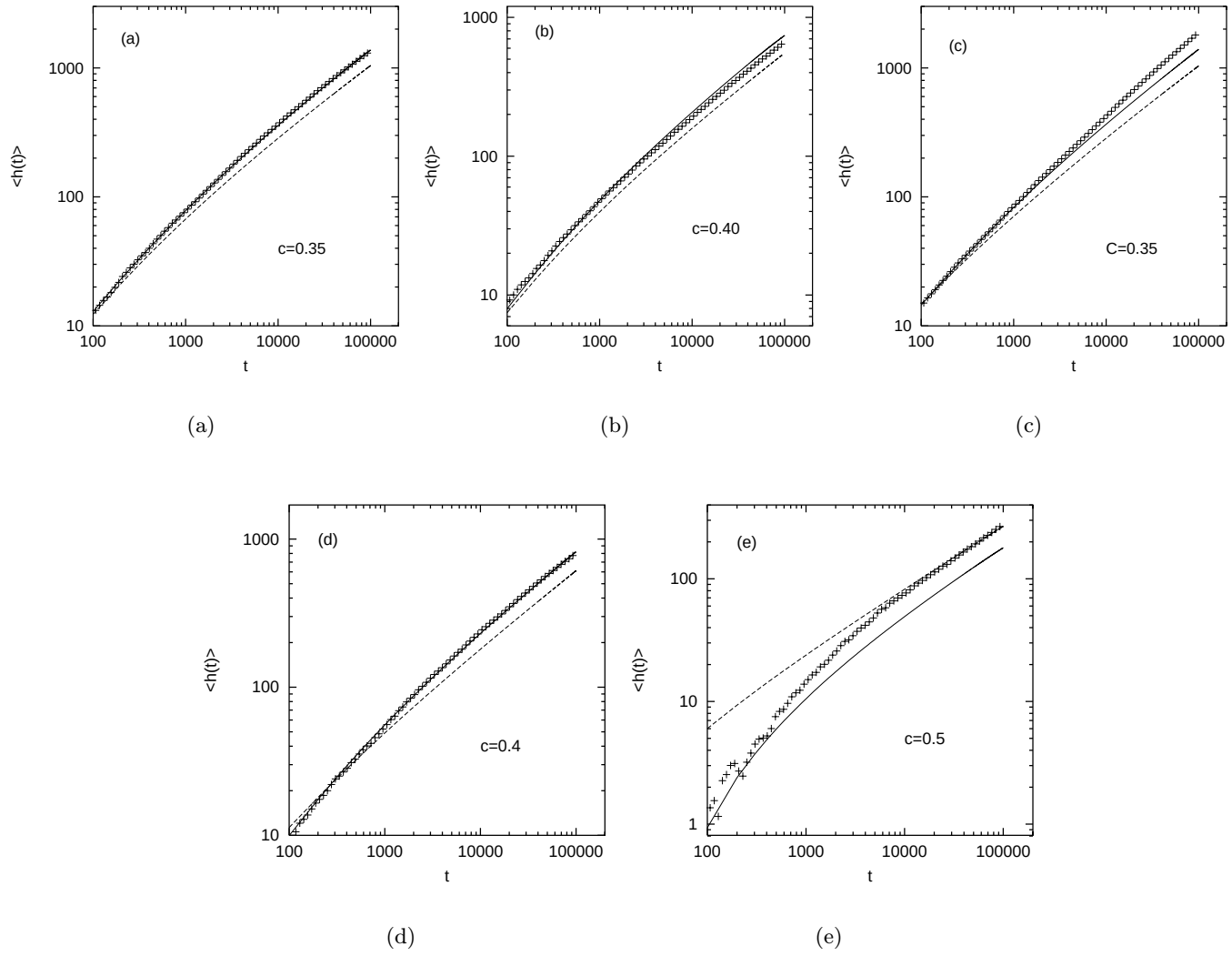

Fig. 5. The interface position $h(t)$ calculated by the analytical approximation with effective diffusion coefficients D_S^e and D_L^e (solid lines) and bare diffusion coefficients D_S and D_L (dashed lines) compared with the Monte-Carlo results (symbols) for (a-b) symmetric diffusion and (c-e) one-sided models. Concentrations are (a) $c = 0.35$, (b) $c = 0.40$,(c) $c = 0.35$, (d) $c = 0.40$, and (e) $c = 0.50$.

5 Conclusion

We study the propagation of the solidification front of the AB binary alloy growing from its melt in a one dimensional model, which should remain relevant also in more realistic two and three-dimensional systems within certain parameter-ranges [5]. The Monte-Carlo simulation shows that in the one-phase region the alloy grows steadily with a velocity controlled solely by kinetics. In the two-phase region the observed anomaly for the diffusionless growth is cured by the diffusion of atoms and the $t^{1/2}$ growth law is confirmed at least in the range of concentration $0.401 = c_3 < c < 0.5$. We can quantitatively explain this behavior by an approximate analytical treatment leading to two types of bare and effective diffusion coefficients.

Because of the limited simulation time we can only suggest two possible scenarios for the general long time asymptotic behavior $\langle h(t)\rangle$ of the interface movement. The first scenario is that in the two-phase region the behavior is governed by an effective diffusion equation (Eqs. (9–13)). For arbitrary but non-zero bare diffusion constants D_S and D_L the interface position $\langle h(t)\rangle$ obeys the following time-dependence. For a point exactly on the solidus or liquidus line (see also [14]) one obtains:

$$\langle h(t)\rangle \sim t^{2/3} \quad \text{for} \quad c = C_{S(L)}.$$

Inside the two-phase region we have the usual diffusion law

$$\langle h(t)\rangle \sim t^{1/2} \quad \text{for} \quad C_S < c < C_L,$$

within this scenario. The concentration point c^* where solidification is replaced by melting is [3]

$$c^* = (C_S\sqrt{D_S^e} + C_L\sqrt{D_L^e})/(\sqrt{D_S^e} + \sqrt{D_L^e}).$$

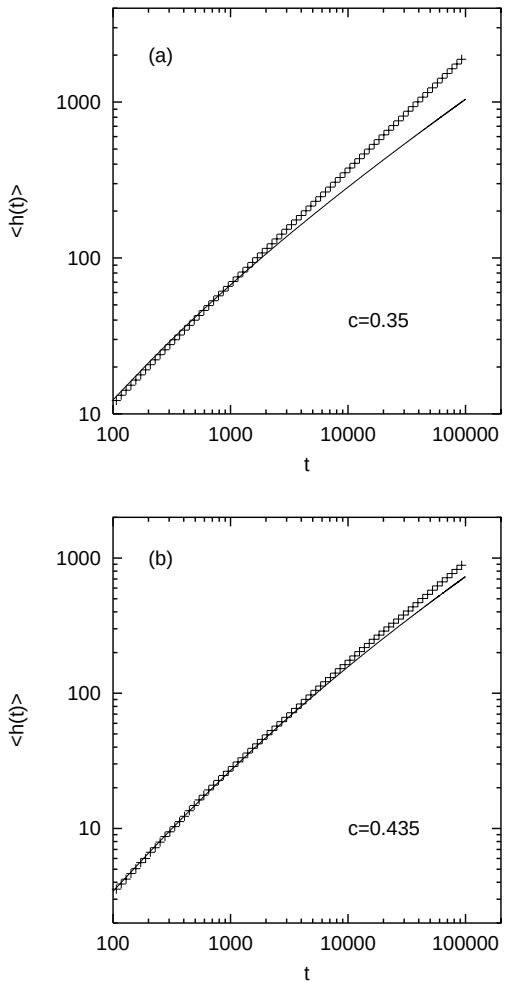

Fig. 6. The interface position $\langle h(t)\rangle$ calculated by the diffusionless Monte-Carlo simulations (symbols) and by the numerical integration with effective diffusion coefficients $D_S^e = D_L^e = 1$ (solid lines). Concentrations are (a) $c = 0.35$ and (b) $c = 0.435$.

We note that this point c^* in general differs from the corresponding point c_0 for the diffusionless process,

$$c_0 = \ln\left(\frac{w_{+A}}{w_{-A}}\right) \ln\left(\frac{w_{+A}w_{-B}}{w_{-A}w_{+B}}\right).$$

For our choice of parameters w, $c_0 = 1/2$ coincides with c^* for the symmetrical diffusional model. This scenario is based on the solution of the effective equations (9–13) where the effective diffusion coefficients are renormalized by correlation effects. This is in agreement with Figures 5a, b, d and e, but in some disagreement with the long-time behavior seen in Figure 5c (and the corresponding value of ν_1 in Fig. 4b for the concentration $c = 0.35$). We should remark that this scenario does not reproduce the limiting case of the diffusionless process where $\langle h(t)\rangle \sim t^{\nu_1}$.

The second scenario is that the asymptotics with diffusion would not be slower than that without diffusion, meaning

$$\langle h(t)\rangle \sim t^{\nu_1} \quad \text{for} \quad \nu_1 > 1/2$$

and

$$\langle h(t)\rangle \sim t^{1/2} \quad \text{for} \quad \nu_1 < 1/2$$

with ν_1 being the anomalous exponent of diffusionless growth. Unfortunately, however, we have no explicit analytical explanation at hand for this second scenario other than the argument, that the faster of two processes running in parallel wins (in contrast to two processes in series, where the slower one is rate-controlling). This second scenario has some support from the long-time behavior of Figure 5c, and the corresponding Figure 4b for the concentration $c = 0.35$, indicating that the otherwise nice agreement of the simulation results with scenario one may be lost for very long simulation times in these parameter ranges. In order to understand which of these scenarios is correct for the diffusional process or if still some other nontrivial exponents can appear in the range where the diffusionless exponent is $\nu_1 > 1/2$, further numerical and analytical efforts will be necessary.

Y.S. and H.M-K. gratefully acknowledge support from the Germany-Japan exchange program of the Japanese Society of Promotion of Science and the Deutsche Forschungsgemeinschaft. We also appreciate support by Volkswagen-Foundation and Russian Fund for Fundamental Research (Project 98-02-16249).

References

1. D.E. Temkin, J. Cryst. Growth **5**, 193 (1969).
2. D.E. Temkin, Dokl. Akad. Nauk SSSR **206**, 27 (1972) [Sov. Math. Dokl. **13**, 1172 (1972)].
3. D.E. Temkin, Kristallografiya **17**, 77 (1972) [Sov. Phys. Crystallogr. **17**, 60 (1972)].
4. Y. Saito, N. Tanabe, D. Temkin, Phys. Rev. E **48**, 2028 (1993).
5. X. Feng, E. Brener, D. Temkin, H. Müller-Krumbhaar, Y. Saito, to be published.
6. J. Bernasconi, W.R. Schneider, J. Phys. A **15**, L729 (1982).
7. B. Derrida, Y. Pomeau, Phys. Rev. Lett. **48**, 627 (1982).
8. B. Derrida, J. Stat. Phys. **31**, 433 (1983).
9. C. Asulangul, M. Barthelemy, N. Pottier, D. Saint-James, J. Stat. Phys. **59**, 11 (1990).
10. J.P. Bouchaud, A. Georges, Phys. Rep. **195**, 127 (1990).
11. J.P. Bouchaud, A. Comtet, A. George, P. Le Doussal, Ann. Phys. **201**, 285 (1990).
12. Ya. G. Sinai, in *Mathematical Problems in Theoretical Physics* edited by R. Schneider, R. Seiler, P. Uhlenbrock, Lecture Notes in Physics Vol. 153 (Springer, Berlin, 1982), p.12.
13. T. Harms, R. Lipowsky, Phys. Rev. Lett. **79**, 2895 (1997).
14. A.R. Umantsev, Kristallografiya **30**, 153 (1984); [Sov. Phys. Crystallogr. **30**, 153 (1984)].